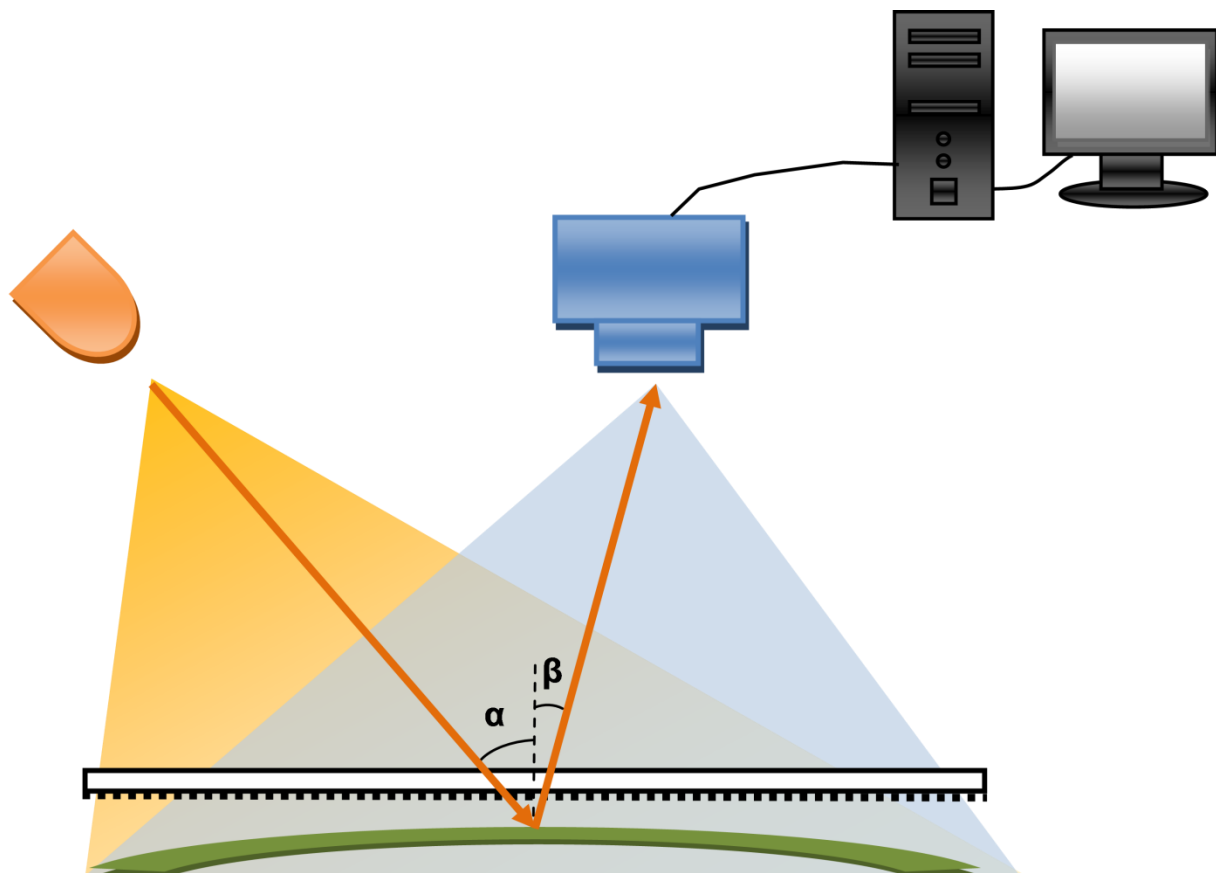




AKROMETRIX OPTICAL TECHNIQUES AND ANALYSES 101



Akrometrix Proprietary Information

No reproduction, adaptation, or translation without prior written approval.

Warranty

The information contained in this document is subject to change without notice.

Akrometrix makes no warranty of any kind with respect to this information.

Akrometrix shall not be liable for any direct, indirect, incidental, consequential, or other damage alleged in connection with the furnishing or use of this information.

Trademark Credits

Microsoft®, Windows®, Excel®, and Notepad® are registered trademarks of Microsoft Corporation.

TherMoiré® is a registered trademark of Akrometrix, LLC.

Contents

1 Shadow Moiré and Fringe Projection.....	4
1.1 Shadow Moiré Basics	4
1.2 Fringe Projection Basics	5
1.3 Comparing Shadow Moiré and Fringe Projection	7
1.4 Phase Shifting Analysis	8
1.5 Unwrapping and Displacement Calculation	11
1.6 Reference Plane for Transformation	12
1.7 Quality Mapping	14
1.8 Noise Filtering	15
1.9 Grating Compensation for Shadow Moiré	19
1.10 Gauges.....	19

1 Shadow Moiré and Fringe Projection

Shadow moiré and fringe projection are two different optical metrology techniques that can be used to measure out-of-plane displacement on diffuse surfaces. Most Akrometrix products are based on these two optical techniques. In this manual, the principles of shadow moiré and fringe projection are described first. Then, a data collection and analysis method called phase shifting, which is used for both techniques, is introduced. Finally, some common data analysis approaches are presented. This document is intended for use with Studio 8.3.

1.1 Shadow Moiré Basics

Shadow moiré is based on the geometric interference of a physical grating (reference grating) and its shadow projected on a sample surface. A typical implementation of a shadow moiré system and its principle is shown in **Figure 1.1**. The primary optical elements are a white light source, a grating suspended above a sample, and a camera (with lens) interfaced with a computer. The grating is a piece of clear, low CTE glass with a patterned chrome film on the bottom surface.

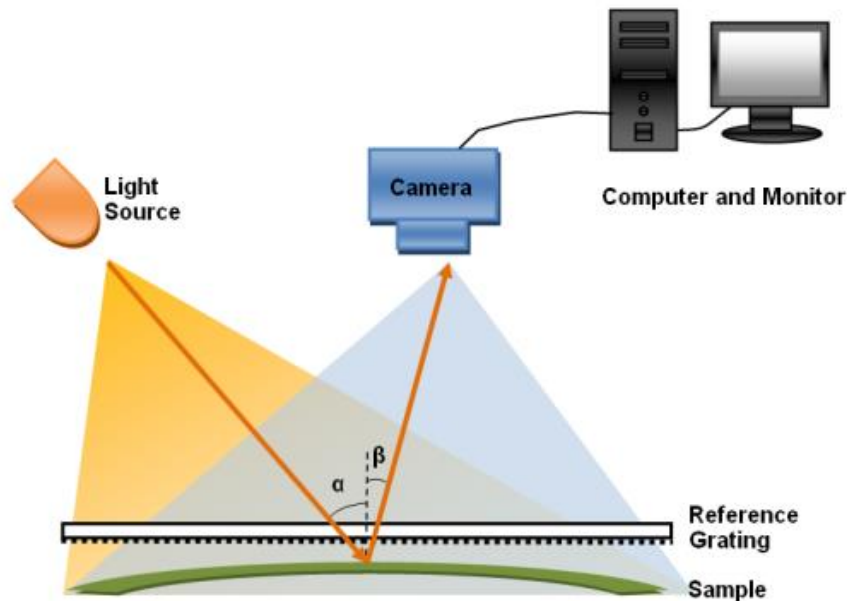


Figure 1.1 Shadow Moiré System Diagram

As shown in **Figure 1.1**, light passes through the reference grating at an oblique angle α (typically around 45°), and casts a shadow of the grating on the sample. The shadow grating will be distorted by the out-of-plane shape of the surface. When this shadow grating is observed through the reference grating at a different angle β (typically 0°), the overlap of the shadow and real gratings forms moiré fringes that represent the topology of the surface. If the specimen is flat and parallel to the reference grating, no moiré pattern is observed. However, when the surface of the specimen is warped, a series of dark and light fringes (moiré fringes) are observed by the camera. An example of a moiré fringe pattern is shown in **Figure 1.2**.

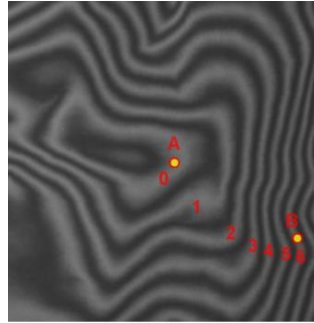


Figure 1.2 Moiré Fringe Pattern

Each successive fringe represents a height change of the sample surface, defined as the height-per-fringe, or Fringe Value. The Fringe Value, w , can be calculated from the following equation:

$$w = \frac{p}{\tan \alpha + \tan \beta} \quad (1)$$

where p is the pitch of the grating (center-to-center distance between lines), α is the angle of illumination, and β is the angle of observation. For example, assume the angle of illumination is approximately 45° and the angle of observation is approximately 0° . If a 100 line per inch (lpi) grating is used, p is 10 mils (0.01 inches), then $w = p = 10$ mils height change per fringe. From **Equation 1**, we can see that the resolution of the shadow moiré system is dependent on the pitch of the grating, the illumination angle, and the observation angle. Sample size does not affect the measurement resolution. Therefore, when α , β , and the grating pitch are fixed, shadow moiré offers a constant resolution for samples with a large range of dimensions.

The relative height between any two points in the fringe image can be calculated by counting the number of fringes between them and multiplying by the Fringe Value. This is illustrated in **Figure 1.2**, where the relative height of points A and B is calculated by counting 6 complete fringes between them and multiplying by w . The moiré fringes from A to B may not be distributed uniformly, but each fringe represents the same height value. In **Figure 1.2**, there is no way to tell whether B is higher or lower than A from the fringe pattern alone. In addition, it is difficult to locate the points to the fractional part of one fringe, especially when the fringe shape is complicated. This is discussed in **Section 1.4** on phase shifting.

1.2 Fringe Projection Basics

The fringe projection technique measures surface contour by projecting fringes onto a sample and then observing the fringe distortion from another angle of view. The projected fringes are modulated by the shape of the sample and can be analyzed to construct the contour of the sample. The principle of the fringe projection technique is shown in **Figure 1.3**. Fringe patterns can be generated electronically by a digital projector or by projecting light through a physical grating. **Figure 1.3** demonstrates a fringe projection system that contains a white light source, a glass grating, a projection lens, and a camera (with lens) interfaced with a computer. The fringe pattern on the grating is projected onto the sample surface through a projection lens at an angle α to the sample

surface normal. The fringes on the sample surface can be viewed by a camera at another angle β relative to the surface normal. The larger the angle between the projection and observation directions is, the higher the measurement sensitivity. When $\alpha + \beta$ equals 90° , the sensitivity reaches its maximum value. However, larger angles will produce shadows on the side of features furthest from the projection source. These shadows will result in missing data in a phenomenon known as *occlusion*.

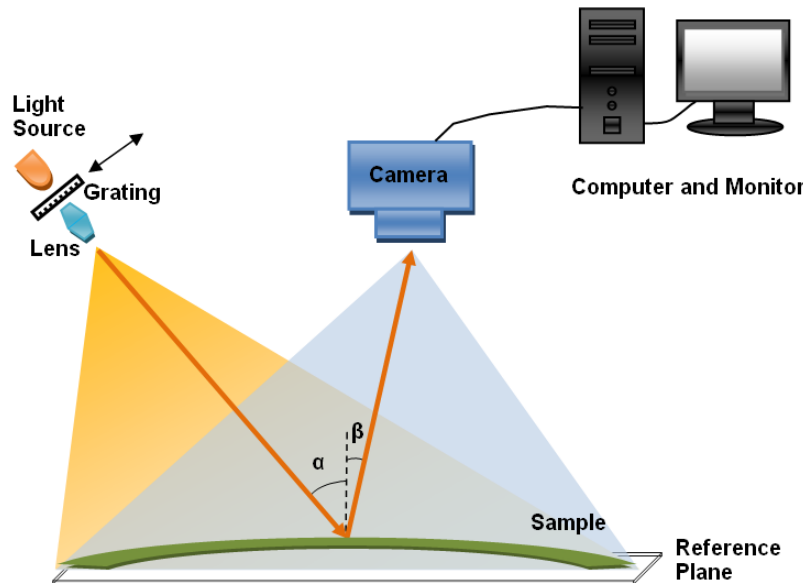


Figure 1.3 Fringe Projection System Diagram

Figure 1.4 shows an image of the projected fringe pattern on a sample. Unlike shadow moiré, the fringes themselves do not represent the height change of the sample surface. Instead, it is the amount of fringe distortion relative to the same fringe on a reference plane (as shown in **Figure 1.5**) that represents the height change. The fringe change relative to that of the reference plane can be determined by subtracting the reference plane phase map from the sample surface phase map. As such, the phase information of a sample surface is meaningless unless the system has a reference plane image to subtract with. The reference plane image is taken during calibration, before any real surface measurements are taken. Details about phase analysis from fringe images will be introduced in **Section 1.4** and **1.5**. For data analysis, reference plane data will be taken into consideration by the software automatically.

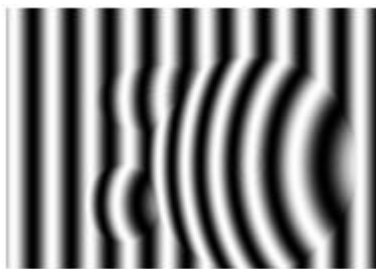


Figure 1.4 Projected Fringe Pattern

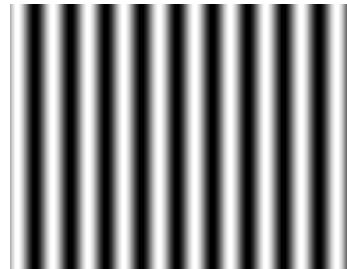


Figure 1.5 Reference Plane Image

The height-per-fringe-change, w , can be calculated using the same **Equation 1** described in **Section 1.1**. In this equation, α still denotes the angle of illumination and β

stands for the angle of observation. However, p is now the pitch of the projected fringe on the sample instead of the pitch of the physical grating. For a fixed grating, p can be different when the same number of lines is projected on a different field of view. Therefore, when α and β have been selected, fringe projection resolution will scale with the FOV. The measurement resolution will reduce when FOV increases.

1.3 Comparing Shadow Moiré and Fringe Projection

1.3.1 Common Features

Both techniques are non-contact and full-field optical methods for measuring relative vertical displacement of continuous, opaque surfaces. They both have several significant advantages over scanning methods, where a height measurement sensor with a single point or a structured line of light is translated on a stage across a sample.

- High Speed – a large number of data points (depending on the number of camera pixels) can be taken rapidly.
- Non-Contact – the sample is isolated from sensitive optical, electronic, and mechanical components of the measuring system, so the sample may be subjected to varying temperature and other environmental conditions.
- Simple – relatively few moving parts are required.

In order to clearly view a fringe pattern, the sample surface must scatter light diffusely. Transparent, specular, and translucent surfaces are problematic since the fringe pattern as seen by the camera is not clearly defined or has a low contrast.

In addition, the measurement surface should be continuous with no abrupt steps or sharp edges because of the periodic nature of the fringes. At a sharp step in height, for example, the fringes associated with the change in height would be compressed into such a narrow region that the camera cannot resolve and accurately count them.

1.3.2 Different Applications

Because the out-of-plane resolution of shadow moiré is primarily a function of grating pitch, this technique can be scaled to relatively large samples without resolution loss. However, shadow moiré becomes impractical as sample size decreases, especially below 3 mm. When camera image pixel pitch approaches the grating pitch, the reference grating lines can be observed in the camera image and introduce an aliasing error in the displacement data. A finer pitch grating can be used to overcome this problem, however, the tradeoff will be a reduced working distance between the sample and the grating.

On the other hand, the out-of-plane resolution of fringe projection is dependent on the FOV. With different FOV sizes, the projected fringe pitch will be different, and so will the resolution. When sample size drops to 10 mm or smaller, the fringe projection technique has comparable out-of-plane resolution to shadow moiré but significantly finer XY imaging resolution. Since there is no grating placed over the sample, there are no grating lines to create the aliasing problem as in shadow moiré.

In summary, each technique has its own favorable applications. In general shadow moiré is robust and copes well with larger sample sizes; Fringe projection is better suited to resolving fine surface features on smaller samples.

1.4 Phase Shifting Analysis

The analysis outlined in **Section 1.1** and **1.2** has three major limitations:

- Fringe analysis along a path cannot determine if the change in height is positive or negative.
- Fringe analysis has relatively low resolution. The relative height between two points cannot be known more accurately than one fringe pitch.
- Fringe analysis is difficult if the illumination or sample surface reflectivity is not of uniform brightness. Fringes can be difficult to separate out from surface features such as solder pads and circuit traces on a PCB sample.

These difficulties make fringe analyses very slow, labor-intensive, and subject to error. In order to address these problems, a phase shifting technique can be used with both optical techniques. In phase shifting, three or more fringe images are obtained as part of each measurement. Between each successive image, the fringes are shifted by a fraction of one fringe period.

For both shadow moiré and fringe projection, the intensity profile of the fringe on the phase-shifted image can be illustrated in **Figure 1.6** and expressed in **Equation 2**.

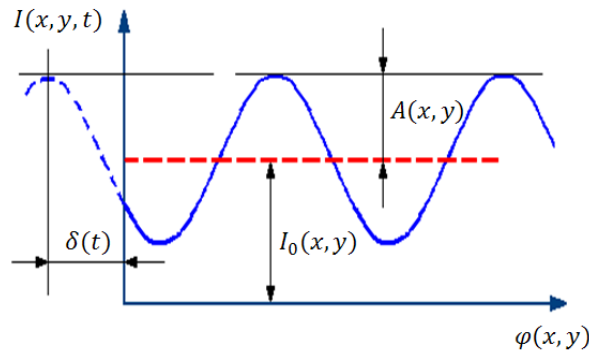


Figure 1.6 Intensity to Phase Function

$$I(x, y, t) = I_0(x, y) + A(x, y)\cos[\varphi(x, y) + \delta(t)] \quad (2)$$

Equation 2 is effective for each point on the sample surface, where a point is defined as the area imaged by one camera pixel. In this equation, $I_0(x, y)$ is the average intensity, and $A(x, y)$ is the fringe amplitude at that pixel. They are dependent on the level of illumination, surface reflectivity, and other factors such as the viewing angle. The term $\delta(t)$ is a known introduced phase shift. Lastly, $\varphi(x, y)$ is the phase that is related to surface height and the quantity we desire to measure.

1.4.1 Four-step (Fixed Phase Shift) phase shifting algorithm

Among many of the phase-shifting algorithms, a four-step phase shifting algorithm is relatively simple, fast and insensitive to phase shifting error. It is commonly used by both Shadow Moiré and Fringe Projection techniques.

In the four-step phase (Fixed Phase Shift) shift algorithm that is used by Akrometrix systems, four fringe patterns are generated sequentially. They can be expressed as:

$$I_1(x, y) = I_0(x, y) + A(x, y)\cos[\varphi(x, y) + 0^\circ] \quad (3)$$

$$I_2(x, y) = I_0(x, y) + A(x, y)\cos[\varphi(x, y) + 90^\circ] \quad (4)$$

$$I_3(x, y) = I_0(x, y) + A(x, y)\cos[\varphi(x, y) + 180^\circ] \quad (5)$$

$$I_4(x, y) = I_0(x, y) + A(x, y)\cos[\varphi(x, y) + 270^\circ] \quad (6)$$

By combining **Equations 3** through **6**, $\varphi(x, y)$ can be solved for the following:

$$\varphi(x, y) = \tan^{-1} \left[\frac{I_4(x, y) - I_2(x, y)}{I_1(x, y) - I_3(x, y)} \right] \quad (7)$$

In **Equation 7**, the contrast terms $I_0(x, y)$ and $A(x, y)$ do not appear, which indicates that the illumination, or surface nonuniformity, does not affect signal phase. Therefore we can overcome difficulty **c**, above, by canceling out the illumination and surface feature factors from the fringe patterns. In addition, phase shifting makes use of the gray level information contained in the fringe pattern images so that it resolves the fractional fringe order. If we present phase values from 0 to 4095 gray levels with a 12-bit system, the fractional fringe to 1/4096 can be theoretically resolved. In practice, a variety of other factors such as phase stepping precision affect resolution at this scale, and an experimental resolution of 1/100 of a fringe order is widely accepted. Therefore, this technique addresses difficulty **b**.

When phase shifting analysis is performed for each pixel in the intensity images, we can display the resulting phase values as a phase image, as shown in **Figure 1.9**, where the brightest points have a phase value of 2π and the darkest points have a phase value of zero. Although the phase image shows patterns similar to the source intensity images, the phase fringes are different in one important respect. Phase changes monotonically from black to white across one fringe and then changes abruptly from white to black at the fringe boundary. In other words, the phase image fringes have directionality, which the original intensity fringes do not. Phase, and therefore height, is changing along a path following the gradient from black to white. The abrupt change from white to black represents the phase resetting from 2π to 0 at the fringe boundary, but not a change in height. In this way, phase shifting analysis also resolves difficulty **a**. High points and low points can be determined by a user or by the computer automatically from the phase image.

To perform phase shifting, the grating or sample support needs to be attached to a high-resolution stage driven by a motor. For shadow moiré systems, either the grating or the sample can be translated vertically with respect to each other to generate phase shifting on the sample. For fringe projection systems, the grating is translated along its

own plane, as shown with an arrow in **Figure 1.3**. A typical phase shift amounts to one-fourth of the grating pitch for the four-step phase shifting method.

1.4.2 Random phase shifting algorithm

The four-step phase shifting algorithm introduced in **Section 1.4.1** requires each phase shift step to be exactly one-fourth of the grating pitch or 90° in the **Equations 3** through **6**. In practice, there are many factors, such as mechanical movement errors, vibrations, and thermal jitter that can contribute to phase shifting error; these errors will make the actual phase shift deviate from 90° . If the phase shift error is severe, the phase image will look banded and ripples will appear on the 3D surface (**Figure 1.7**). In this case, we can apply the random phase shifting algorithm.

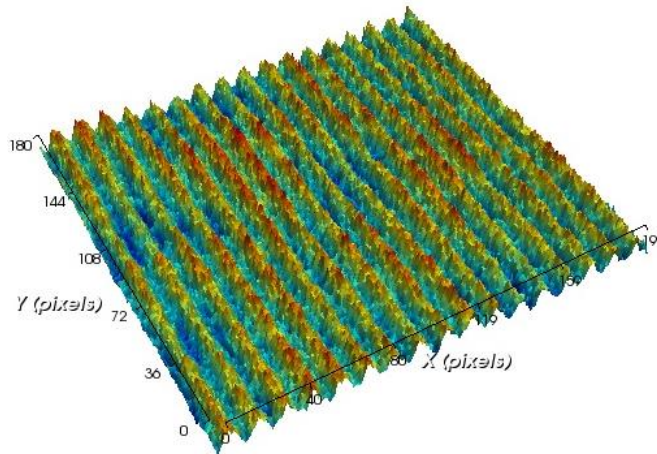


Figure 1.7 Phase Shifting errors due to vibration effects using Fixed Phase Shift algorithm

The random phase shifting algorithm is based on a least-squares iterative procedure. It extracts each actual phase shift from the measurement and applies them to the phase calculation. Because accurate phase shift amounts are found, the phase image and 3D result will be more accurate than if calculation of phase is based on the assumption of equal phase shifts. **Figure 1.8** shows the phase image and 3D result of the random phase shifting algorithm for the same measurement shown in **Figure 1.7**.

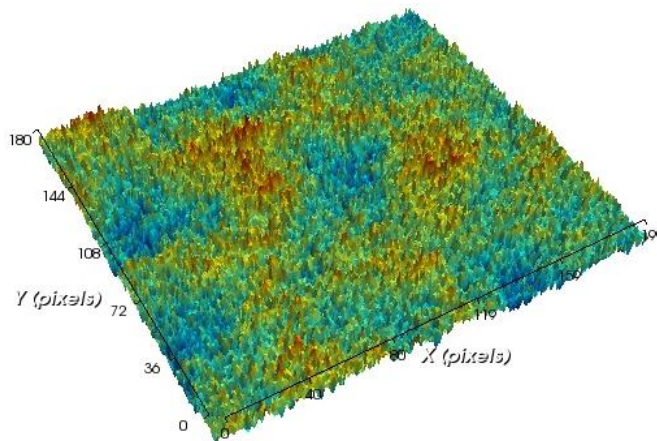


Figure 1.8 Phase Shift errors corrected by using Random Phase Shift algorithm

Since the random phase shift algorithm is an iterative method based on the whole ROI, the computation speed can be slow or the result may not be convergent if the data is noisy or has local dark areas that are not completely masked out. In general, the Fixed Shift four-step phase shift algorithm is used for both Shadow Moiré and Fringe Projection techniques because it is fast and robust. The Random Phase Shift algorithm is only used when the phase shift error cannot be predicted or compensated by any other means.

1.5 Unwrapping and Displacement Calculation

A typical phase image has an abrupt grayscale change periodically as shown in **Figure 1.9** and is defined as a “wrapped” phase image. This is because phase is computed from an arctangent function (see **Equation 7**) which has a range between 0 and 2π if signs of the numerator and denominator are known.

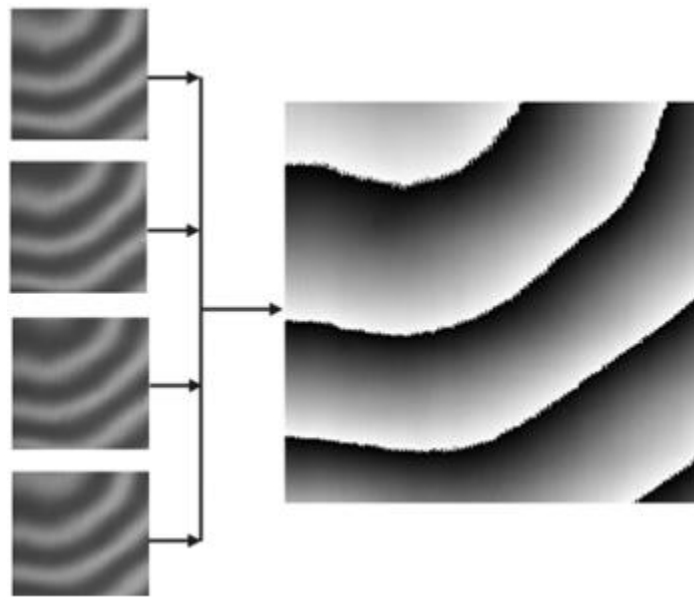


Figure 1.9 Combining Four Intensity Images into One Phase Image

Before converting the phase image to displacement data, an additional analytical step called “unwrapping” is used to generate a continuous phase map image. An example of one-dimensional unwrapping is illustrated in the following figures. Phase along the horizontal line in **Figure 1.10** is graphed in **Figure 1.11**, where it shows multiple discontinuities. Unwrapping along this line converts the discontinuous curve to a smooth continuous curve by adding or subtracting multiples of 2π to each segment.



Figure 1.10 Wrapped Phase Image

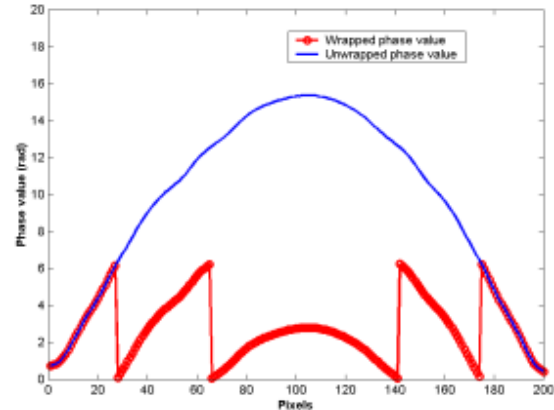


Figure 1.11 Cross Section of Phase Image Before and After Unwrapping

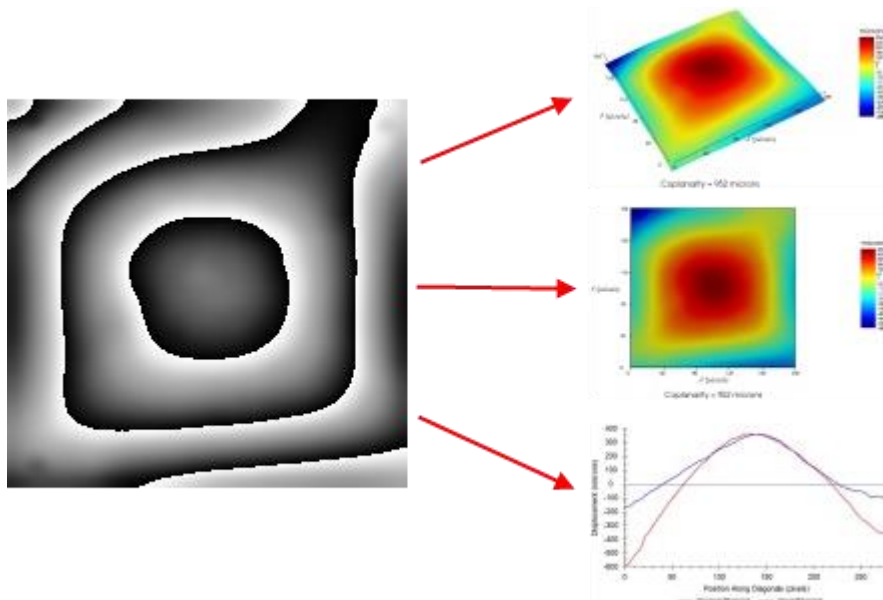


Figure 1.12 Unwrapped Phase Image and Converted Displacement Graphs

After unwrapping, the phase values are multiplied by a calibrated constant, the Fringe Value, to give the displacement data at each point. **Figure 1.12** illustrates several display formats available with the Akrometrix Surface Analysis program, which automates the unwrapping and plotting of phase images. For fringe projection, reference plane data is subtracted from the unwrapped phase data before multiplying the fringe value.

1.6 Reference Plane for Transformation

In order to display the displacement data, the user may define a coordinate system with a zero reference plane. This reference plane is different from the reference plane data used for fringe projection measurement. The surface contour can be transformed (rotated and/or translated) mathematically into the coordinate system without changing the shape of the surface.

The Surface Analysis program provides the user with several options for defining the zero reference plane:

None: The displacement data is not transformed and thus the reference plane is parallel to the grating. The zero value on the data does not correspond to any specific feature of the displacement surface.

LSF: The displacement data is transformed so that the zero reference plane is the best fit plane calculated from all displacement points.

LSF Low 0: LSF transformation option with the lowest displacement point set equal to zero (all others are positive displacement values).

LSF High 0: LSF transformation option with the highest displacement point set equal to zero (all others are negative displacement values).

Three Point: The displacement data is transformed so that the zero reference plane is defined by three corners (upper left, lower left, and upper right).

Four Point: The displacement data is transformed so that the zero reference plane is the LSF fit plane calculated from all four corners.

The values of the individual data points change as a function of transformation (choice of reference plane), so gauges (e.g. coplanarity) and other calculated values are also a function of this transformation. **Figure 1.13** shows a two-dimensional example of calculating coplanarity value (see definition in **Section 1.10.1**). The coplanarity results of the same sample data could vary depending on the reference plane selection.

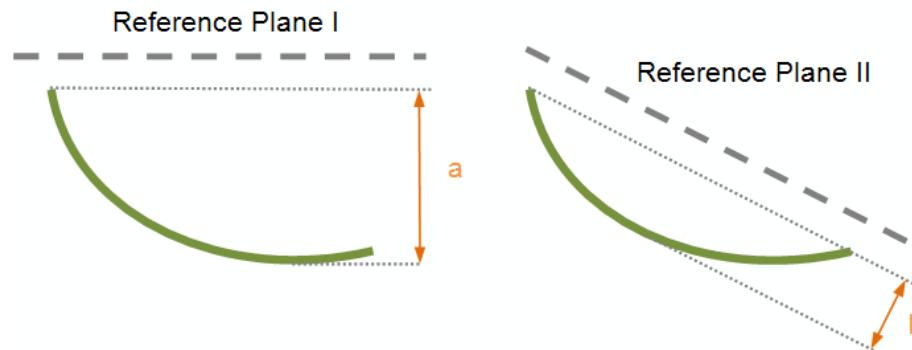


Figure 1.13 Coplanarity Values of the Same Sample Based on Different Reference Planes

Even when the same reference planes are selected, the gauge values can be different when a sample is positioned at different angles with respect to the reference plane (e.g. grating). See **Figure 1.14**.

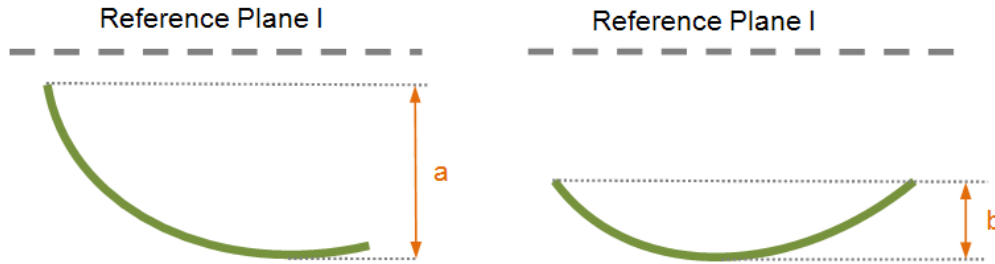


Figure 1.14 Coplanarity Values of the Same Sample Placed at Different Angles

In order to achieve consistent warpage gauges, an LSF based reference plane is recommended. This reference plane is based on the sample data itself and is invariant to sample transformation. See **Figure 1.15**.

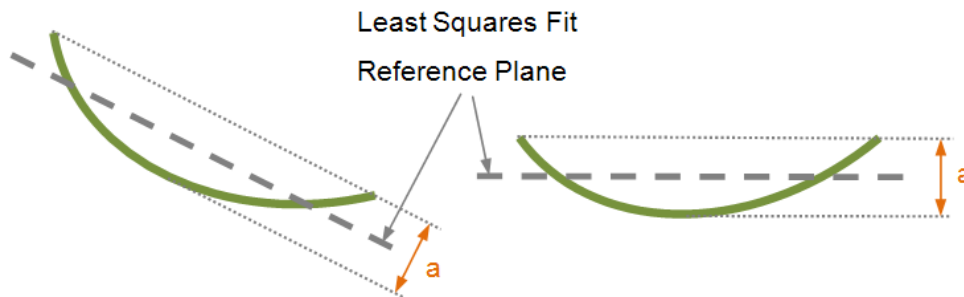


Figure 1.15 Coplanarity Values of a sample based on an LSF Reference Plane

1.7 Quality Mapping

A quality map is a matrix of values that define the quality or “goodness” of each pixel of the given phase data. A quality map allows the system to automatically recognize regions within the image which may cause problems in the analysis and exclude those data points from the analysis.

The quality map is defined by the phase amplitude term $A(x, y)$ in **Equation 2** and can be derived from **Equations 3** through **6** as follows:

$$A(x, y) = \frac{1}{2} \sqrt{(I_4(x, y) - I_2(x, y))^2 + (I_3(x, y) - I_1(x, y))^2} \quad (8)$$

The phase amplitude indicates the “goodness” of the phase data at that specific point. A larger phase amplitude value indicates better fringe brightness.

In the Surface Measurement software, quality mapping is activated when the Phase Amplitude Threshold is enabled (Refer to the **Surface Measurement User Manual**). Pixels whose phase amplitude is less than a preset threshold value are masked and will show up as holes in the resulting displacement plot. As of Studio 8.0, the Phase Amplitude Threshold can also be adjusted after acquisition during analysis in Surface Analysis (Refer to the **Surface Analysis User Manual**).

Selecting a threshold is a user judgment based on experimental conditions (lighting, sample surface features, etc.). **Figure 1.16 - Figure 1.19** shows an example of generating a phase image using different threshold values.

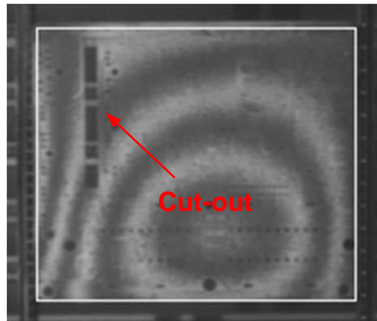


Figure 1.16 PCB with Cut-out

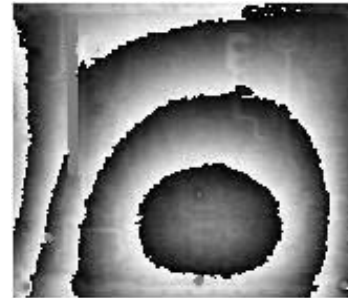


Figure 1.17 Good Threshold (3)

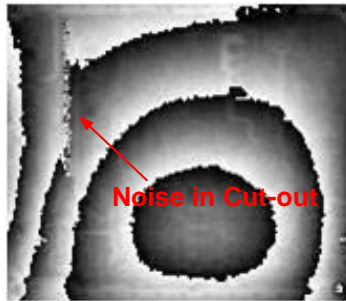


Figure 1.18 Low Threshold (1)

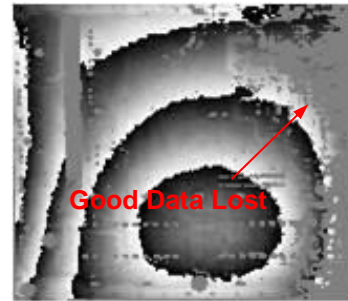


Figure 1.19 High Threshold (20)

The measured sample is a PCB board with a cut-out on the left side as shown in **Figure 1.16**. The cut-out region does not have fringes because there is no surface to reflect any light. When a typical phase amplitude threshold value (2-5 for 8 bit phase, or 16-40 for 12 bit) is applied, the cut-out region will be masked out automatically by the software (**Figure 1.17**). If the threshold is too low, invalid pixels with noise can be left over in the phase image (**Figure 1.18**). When this region is used to guide a phase unwrapping algorithm, these low-quality phase values can corrupt the unwrapped solution. On the other hand, if the threshold is too high, valid data can be masked out (**Figure 1.19**). Regions within the phase image become isolated from one another, which can cause unwrapping errors as well. The threshold values are set based on analysis and experience. The user is able to adjust these values to better satisfy different applications.

1.8 Noise Filtering

The measurement data from Akrometrix equipment, like all other measurement systems, is subject to experimental noise (camera noise, electrical interference, digitization noise, etc.). Typical warpage gauges, such as bow, twist, and coplanarity (**Section 1.10**), are extremely sensitive to this noise. For example, coplanarity is the difference between the highest and lowest points in the entire data set. As a result, a single outlier data point can dominate the results. Therefore, noise filtering can make gauge values that rely on only a small number of data points more repeatable from measurement to measurement. For this reason, Akrometrix provides three types of noise filters to improve gauge repeatability.

1.8.1 Phase Smoothing

Phase smoothing is a filtering algorithm applied to the phase image. The smoothing function is directly applied to several intensity images (where the sharp $0 - 2\pi$ transitions do not show) derived from the phase image. For each intensity image, the intensity value at each pixel is replaced by a weighted average of itself and the pixels surrounding it in a 5 by 5 block of pixels, called a weighted kernel. At the two rows or columns near an edge, a flat LSF regression method is implemented to get a filtered value for those pixels. After each intensity image is smoothed, the phase image is retrieved from the smoothed intensity images. **Figure 1.20** and **Figure 1.21** shows a phase image before and after the phase smoothing algorithm is applied. It can be seen that the smoothed phase image has smoother fringes and less noise.



Figure 1.20 Phase Image Before Smoothing



Figure 1.21 Phase Image After Smoothing

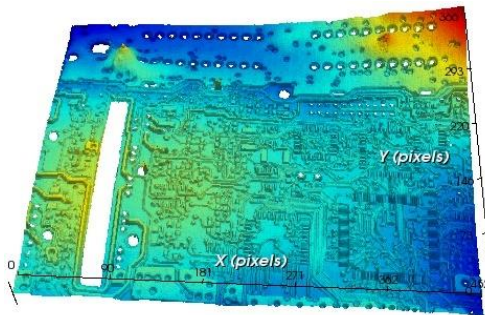


Figure 1.22 3D Displacement Before Phase Smoothing

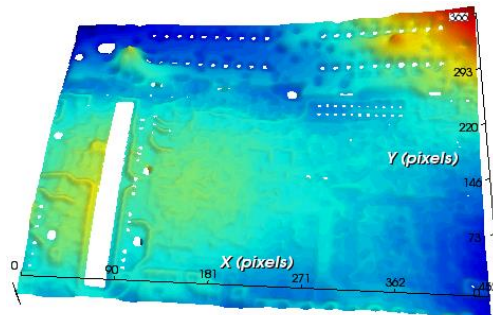


Figure 1.23 3D Displacement After Phase Smoothing

Choosing whether to use a smooth filter or not depends on the nature of the sample and the requirements of the measurement. Filtering reveals the large-scale curvature of the sample and usually improves the repeatability of gauge calculations. **Figure 1.22** and **Figure 1.23** show the 3D surface plots of the phase image used in **Figure 1.20** and **Figure 1.21**. As expected, the smoothed data shows more general shape but washes out fine surface features.

1.8.2 Displacement Smoothing

Phase smoothing may cause errors or artifacts on the 3D surface when applied to images where the fringes are very tightly spaced or at boundaries of masked regions.

Figure 1.24 shows an example of this phenomenon in shadow moiré phase images, where the tightly spaced fringes represent high slope features. After phase smoothing (**Figure 1.25**), some of the fringes are smoothed to the point that they are indistinguishable and result in the 3D surface plot shown in **Figure 1.27**. For phase images generated from the MP10 system, fringes are always distributed closely over the whole phase image field. For DFP measurement images, a phase image is not created. In all cases described above, displacement smoothing is recommended or required instead of phase smoothing.

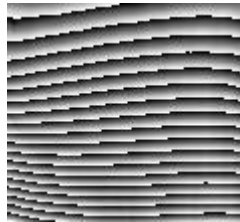


Figure 1.24 Phase Image with Tightly-spaced Fringes Before Phase Smoothing

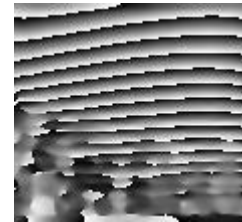


Figure 1.25 Phase Image with Tightly-spaced Fringes After Smoothing

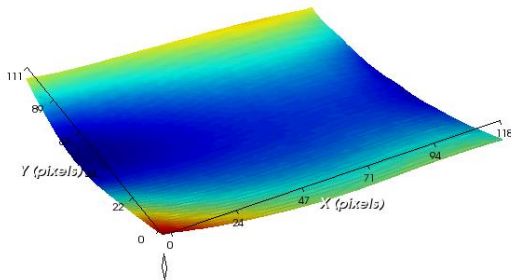


Figure 1.26 3D Surface Plot of a sample with High Slope Features Before Smoothing

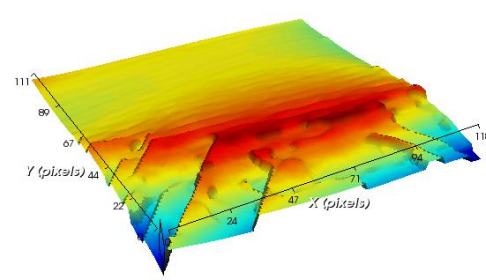


Figure 1.27 3D Surface Plot of a sample with High Slope Features After Smoothing

The default displacement smooth operation applies the same weighted kernel described in **Section 1.8.1** to the 3D displacement data instead of the phase image. Similarly, this filter is useful in reducing analysis error due to noise or fringe miscounting. A custom smooth can also be applied as shown in **Figure 1.28**. The options are described below:

Filter Type: Standard, Gaussian, Median

The Standard filter type will weight the inner 3 x 3 kernel by 2 and the remaining kernel by 1, regardless of the total kernel size set by the user. This is also the default displacement smooth weighting.

The Gaussian filter type will weight each pixel according to a Gaussian function over the user set kernel size.

The Median filter type assigns the center pixel as the median value of all the surrounding pixels in the kernel.

Edge Mode: Mask, LSF

When the smoothing kernel edge hits the edge of the image, half of the kernel cannot be analyzed the same as interior pixels. In Mask mode, the smoothing algorithm will

simply ignore these pixels and exclude them from the smoothed data. In LSF mode, an LSF plane is calculated for these pixels and the data for each pixel up to the halfway point of the kernel is extrapolated from this plane.

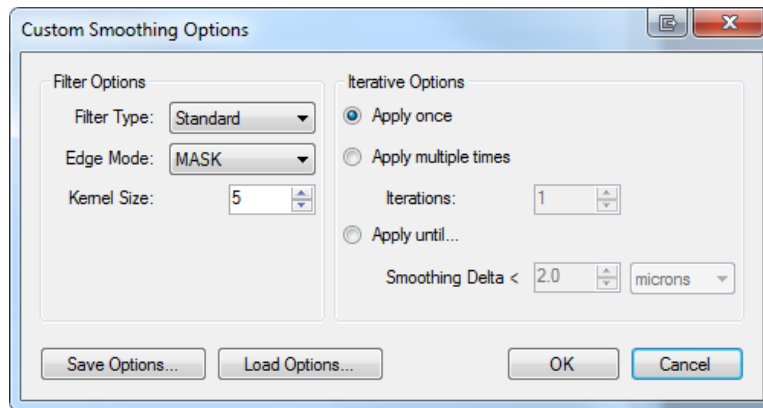


Figure 1.28. Custom Smooth Dialog

Lastly, the chosen smooth operation can be applied once, multiple times, or until the difference between the coplanarity value before and after the smooth is less than the Smoothing Delta.

1.8.3 Surface Fitting

When only the overall shape of the sample is of interest or sample shape disappears in noise, LSF surface-fitting functions can be used. 2nd and 3rd order polynomial surface fit functions (**Equations 9** and **10**) are used for these applications.

$$z(x, y) = a + bx + cy + dxy + ex^2 + fy^2 \quad (9)$$

$$z(x, y) = a + bx + cy + dxy + ex^2 + fy^2 + gx^2y + hxy^2 + ix^3 + jy^3 \quad (10)$$

For a relatively symmetric sample (e.g. single concave or convex surface), a 2nd order surface fit will better match the surface shape. For a more complicated surface, where some local areas are concerned, a 3rd order surface fit will be better suited. **Figure 1.29** through **Figure 1.31** show the difference between these two fitting methods. A warped sample with some local curvatures is shown in **Figure 1.29**. If the user is only interested in the overall shape and intends to ignore local variations, a 2nd order surface fit can be used, which leads to a symmetric surface in **Figure 1.30**. If both global and local areas are concerned, a 3rd order surface fit can be used as shown in **Figure 1.31**.

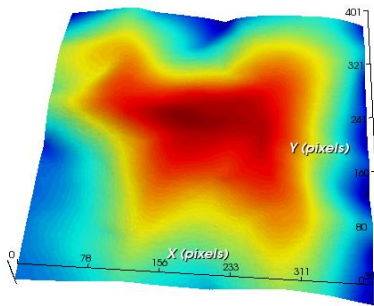


Figure 1.29 3D Surface

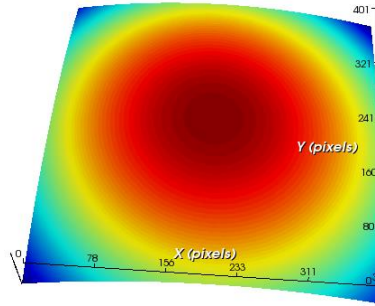


Figure 1.30 2nd Order Surface Fit

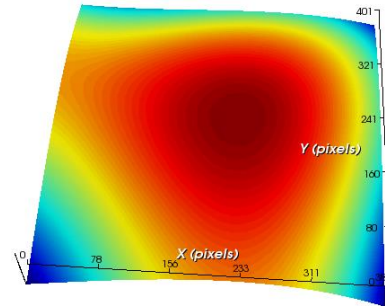


Figure 1.31 3rd Order Surface Fit

1.9 Grating Compensation for Shadow Moiré

Shadow moiré actually measures the gap between the grating and sample, in relative terms. If the grating were perfectly flat, this would be equivalent to measuring the surface contour of the sample. However, real gratings may be non-planar due to manufacturing imperfections and gravitational sag. In general, the effect of grating non-planarity is smaller than the system accuracy specification. Nevertheless, Akrometrix provides custom compensation information for the central region of gratings for users requiring the most accurate measurements of absolute sample curvature.

The grating can be compensated by measuring an optical flat standard. The shape of the measured surface represents the shape of the grating, which can be used as a reference surface for grating compensation. Six parameters are used to define the grating curvature as a 2nd order surface, as in **Equation 9**. These six polynomial coefficients along with the size (width and height) of the compensation region are recorded for the subsequent compensations.

To compensate for the grating curvature, a height correction value is calculated for each point of the phase image based on the six polynomial coefficients. Once the user has specified the phase image's dimensions, the displacement data will be compensated by subtracting the height correction value from each data point in the displacement matrix.

1.10 Gauges

1.10.1 Coplanarity

Coplanarity is the difference between the highest and lowest data points within the Region of Interest. It is always positive and is typically thought to reference an LSF plane of the entire data set. It can reference other planes, however, including no rotation, 3 point, 4 point, and User Defined.

1.10.2 Center Deflection

Center Deflection is an Akrometrix specific function defined as the difference between the average height of the four corners and the height at the center:

$$((Z(\text{UpperLeft}) + Z(\text{LowerRight}) + Z(\text{UpperRight}) + Z(\text{LowerLeft}))/4) - Z(\text{Center})$$

1.10.3 Signed Warpage

Signed Warpage has a magnitude equal to the coplanarity, as defined in **Section 1.10.1**, and a sign (or polarity) determined by a special algorithm to distinguish between convex and concave curvature of the surface. The current implementation uses the curvature of the diagonals AB and CD in **Figure 1.32**, where the endpoints of the diagonals are adjusted to zero and the sign of the Signed Warpage Gauge is the same as the sign of **Equation 11**.

$$\max(AB) + \max(CD) + \min(AB) + \min(CD) \quad (11)$$

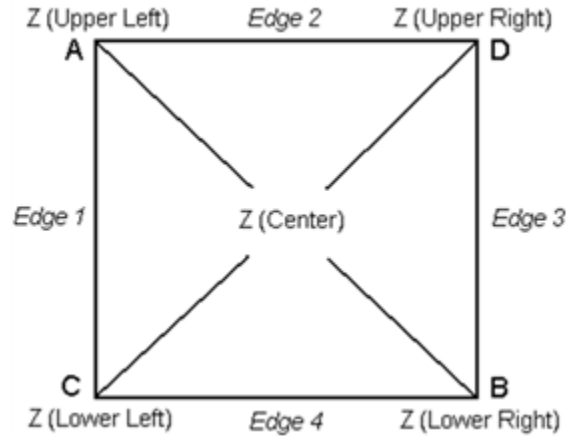


Figure 1.32 Coordinate Definitions for Gauges

1.10.4 Signed Warpage Dead Bug

Signed Warpage Dead Bug has a value equal to $-1 \times \text{Signed Warpage}$. Dead bug gauges flip the concave/convex sign to give warpage values for parts tested with their leads up. This is necessary when comparing warpage values to the JEDEC warpage standard which defines direction with the part leads face down.

1.10.5 Full-field Signed Warpage

Full-field Signed Warpage has a magnitude equal to the coplanarity, as defined in **Section 1.10.1**, and a sign (or polarity) determined by a special algorithm to distinguish between convex and concave curvature of the surface. First, the full surface displacement data is fit to a 2nd order polynomial as in **Equation 9**. Then the polarity is assigned according to the sign of $-(e + f)$, the curvature of the surface along the X and Y axes.

1.10.6 Full-field Signed Warpage Dead Bug

Full-field Signed Warpage Dead Bug has a value equal to $-1 \times \text{FFS Warpage}$. Dead bug gauges flip the concave/convex sign essentially give warpage values for parts tested with their leads up. This is necessary when comparing warpage values to the JEDEC warpage standard which defines direction with the part leads face down.

1.10.7 JEDEC Full-field Signed Warpage

JEDEC Full-field Signed Warpage has a magnitude equal to the coplanarity, just as Full-field Signed Warpage does, but has additional complexity to account for non-square shapes in the shape measurement algorithm. The surface is fit to a 2nd order polynomial just as in Full-field Signed Warpage. The polarity of the shape is then defined as “ $-(em^2 + fn^2)$ ” where m = # of pixels in X and n = # of pixels in Y.



Note: Due to its improved accuracy in determining shape of non-square surfaces, Akrometrix recommends this shape measurement gauge over its predecessor, Signed Warpage and Full-field Signed Warpage.

1.10.8 JEDEC Full-field Signed Warpage Dead Bug

JEDEC Full-field Signed Warpage Dead Bug has a value equal to -1xJFFS Warpage. Dead bug gauges flip the concave/convex sign to give warpage values for parts tested with their leads up. This is necessary when comparing warpage values to the JEDEC warpage standard which defines direction with the part leads face down.

1.10.9 Radius of Curvature (ROC)

The ROC (Radius of Curvature) gauge returns the radius of a sphere used to fit a three-dimensional surface. A positive ROC sign represents a convex curvature (viewed from above) and a negative sign represents concave curvature. The sign definition is in accordance with JEDEC Standard No. 22B112. Radius of Curvature gauge units are always meters.

To calculate the ROC, the 3D surface is first fitted with a sphere using the least squares algorithm. The function of the sphere can be expressed as $(x - a)^2 + (y - b)^2 + (z - c)^2 = r^2$, where (a, b, c) is the sphere center and r is the sphere radius. In this sphere function, we define a constraint as follows: $2(z_{max} - z_{min}) > \min[(x_{max} - x_{min}), (y_{max} - y_{min})]$, which requires that the sample surface should not be warped more than a semi-sphere shape.

The ROC gauge is designed for use with a near-sphere-segment shaped surface where there is only one surface curvature center and all four corners are warped in the same direction. The result will be less accurate shapes that do not meet these criteria such as saddle, cylinder, or asymmetric, nearly flat surfaces.

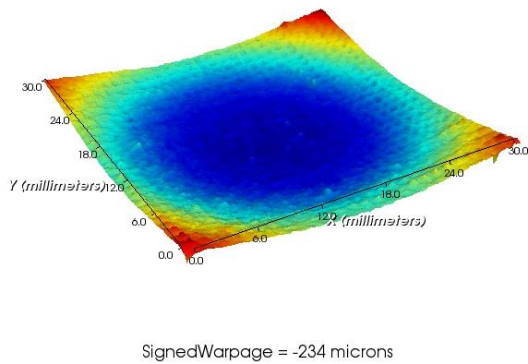


Figure 1.33 Original 3D Surface

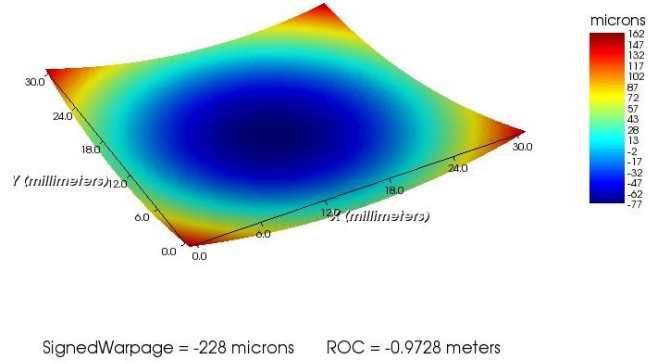


Figure 1.34 Sphere fit of the original surface

1.10.10 Twist

According to the IPC-TM-650 Test Methods manual, *twist* is a measure of the skewness of the opposite edges of a PCB, or equivalently, the extent to which one corner of the PCB lies above or below the plane defined by the other three corners.

For a given ROI, Twist is calculated as:

$$\frac{Z(\text{UpperLeft}) + Z(\text{LowerRight}) - Z(\text{UpperRight}) - Z(\text{LowerLeft})}{\text{Diagonal}} \quad (12)$$

where

Diagonal = physical distance of \overline{AB} or \overline{CD} based on user specified phase image dimensions

Units are scaled such that the result is unit less and reported as a percentage.

1.10.11 Bow

According to the IPC-TM-650 Test Methods manual, *bow* is a measure of the curvature of the sample along its edges. *Bow* is reported to be the maximum bow calculated at any point along the four edges of the ROI.

The bow value at any edge point P along the ROI is determined by:

$$\text{bow}(P) = b/L \quad (13)$$

where b is the displacement measured relative to a chord connecting the edge endpoints and L is the edge length based on user specified phase image dimensions. Units are scaled such that the result is unit less and reported as a percentage.

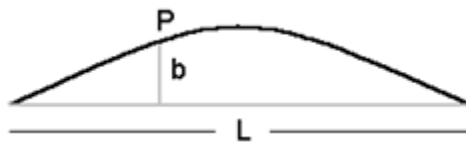


Figure 1.35 Parameter Definitions for Bow

1.10.12 HD Coplanarity

HD Coplanarity is the difference of the median of the top 0.1% and bottom 0.1% of the current data set. Reference plane will affect this gauge just as it does regular Coplanarity.

1.10.13 Signal Strength

Signal Strength (abbreviated SS) is a quantitative measure of the directionality of a surface in relation to warpage direction. This gauge will return results from 0%, or maximally negative, to just over 100%, or maximally positive.

Similar to JEDEC Full-field Signed Warpage, Signal Strength is calculated using a second-order polynomial fit as in **Equation 9**, determined by the following equation:

$$SS = \left| \frac{em^2 + fn^2}{4 \times \text{Coplanarity}} \right| \quad (14)$$

where m = # of pixels in X and n = # of pixels in Y.

1.10.14 Signal Strength Signed Warpage

Signal Strength Signed Warpage, or 3 Signs Warpage, is similar to JEDEC Full-field Signed Warpage, but with additional complexity to account for flat or complex (twisted, saddle shaped, M, W, etc.) shaped surfaces. Its magnitude is equal to the coplanarity and its sign is determined in two steps. First, the Signal Strength of the surface is calculated. If Signal Strength is less than 25%, then the shape is considered transitional – the surface shape deviates too much from the simple concave/convex model that warpage sign typically represents. In this case, the 3 Signs Warpage is reported as TX, where X is the coplanarity. If Signal Strength is greater than 25%, then the sign is determined using the same method as JEDEC Full-field Signed Warpage.



Note: In warpage vs. temperature plots produced in reports, transitional gauge values are plotted with a vertical line from positive to negative on the plot.

1.10.15 Signal Strength Signed Warpage Dead Bug

3S Warpage Dead Bug has a value equal to $-1 \times 3S$ Warpage. Dead bug gauges flip the concave/convex sign to give warpage values for parts tested with their leads up. This is necessary when comparing warpage values to the JEDEC warpage standard which defines direction with the part leads face down.

1.10.16 Die Tilt Angle

Die Tile Angle (abbreviated DTA) measures the maximum angle in degrees of the diagonals of a part. The angle is derived from the ratio of the height difference between diagonal end points to the length of that diagonal. Die Tilt Angle is calculated for both diagonals, with the larger result being used. The calculation is done using this equation:

$$DTA = \sin^{-1} \left(\frac{a - b}{L} \right) \quad (15)$$

where a is the z-value at the higher of the diagonal end points, b is the z-value at the lower of the diagonal end points, and L is the length of that diagonal based on user specified image dimensions.

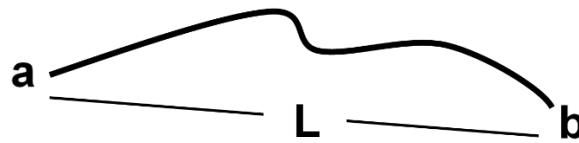


Figure 1.36 Die Tilt Angle Parameter Definitions

1.10.17 Top Left Corner

This gauge reports the z-value of a single pixel at the top left corner of a surface. If the surface does not have data in its top left corner, the diagonal will be checked up to a distance of 5% of the diagonal length in pixels. Beyond this point, the answer will be reported as n/a.

1.10.18 Top Right Corner

This gauge reports the z-value of a single pixel at the top right corner of a surface. If the surface does not have data in its top right corner, the diagonal will be checked up to a distance of 5% of the diagonal length in pixels. Beyond this point, the answer will be reported as n/a.

1.10.19 Bottom Left Corner

This gauge reports the z-value of a single pixel at the bottom left corner of a surface. If the surface does not have data in its bottom left corner, the diagonal will be checked up to a distance of 5% of the diagonal length in pixels. Beyond this point, the answer will be reported as n/a.

1.10.20 Bottom Right Corner

This gauge reports the z-value of a single pixel at the bottom right corner of a surface. If the surface does not have data in its bottom right corner, the diagonal will be checked up to a distance of 5% of the diagonal length in pixels. Beyond this point, the answer will be reported as n/a.

1.10.21 Corner Gap

The corner gap is the largest difference between the values of the four corner gauges. It is always positive.

1.10.22 Center Point

The center point is the z-value of a single pixel at the center of the surface. If the surface has an even number of pixels in any dimension, then the center pixel on the bottom right is used.

1.10.23 Second Order Fit Coefficients

This gauge reports the coefficients for a second order polynomial fit of the surface (**Equation 9**). There are six different reported coefficients: x^2 , y^2 , xy , x , y , and a constant, a . Note that x^2 and y^2 are the same as the values of e and f used to calculate Full-field Signed Warpage, JEDEC Signed Warpage and Signal Strength.